Prepared for the National Institutes of Health
National Institute of Neurological Disorders and Stroke
Division of Stroke, Trauma and Neurodegenerative Disorders
Neural Prosthesis Program
Bethesda, MD 20892

Microstimulation of the Lumbosacral Spinal Cord: Mapping

NIH-NINDS-N01-NS-5-2331

Quarterly Progress Report #8

Period Covered: 1 July, 1997- 30 September, 1997

ORIGINAL

Principal Investigator: Warren M. Grill, Ph.D.[1]
Co-Investigators: Narendra Bhadra, M.D., M.S.[1]
Bernadette Erokwu, D.V.M.[2]
Musa Haxhiu, M.D., Ph.D.[2]
Baoqing Wang, M.D., M.S.[1]

Departments of [1]Biomedical Engineering and [2]Medicine
Case Western Reserve University
Cleveland, OH, 44106-4912

This QPR is being sent to you before it has been reviewed by the staff of the Neural Prosthesis Program.

ABSTRACT

The objectives of this research are to define the anatomical locations of neuronal populations involved in control of genitourinary and motor functions, and to determine the physiological effects of stimulation of these neuronal populations. During this quarter we have made progress on both of these objectives. We continued experiments to map the locations of spinal neurons involved in genitourinary function using expression of the immediate early gene c-fos, and began cell counting to quantify results from mapping experiments. The results of these studies have identified the location of spinal neurons involved in control of micturition and identified target regions for microstimulation. We continued microstimulation studies to map systematically the isometric torques generated about the knee joint by microstimulation of the lumbar spinal cord. In these experiments we also recorded intramuscular electromyograms from four muscles acting at the knee. The results of these experiments suggest that microstimulation can replicate the classical spinal reflexes of flexion withdrawal and crossed extension. Furthermore, out maps in the ventral aspect fo the spinal cord replicate the spatial distribution of flexors and extensors previously demonstrated in anatomical studies.

INTRODUCTION

Electrical stimulation of the nervous system is a means to restore function to individuals with neurological disorders. The objective of this project is to investigate the feasibility of neural prosthetics based on microstimulation of the spinal cord with penetrating electrodes. Specifically, we will use chemical and viral retrograde tracers, stimulation mapping, and field potential recordings to determine the locations in the spinal cord of the neuronal populations that control genitourinary and motor functions in the male cat. We will use selective microstimulation with penetrating activated iridium microelectrodes to determine the physiological effects of stimulation of different neural populations. The results of this project will answer fundamental questions about microstimulation of the spinal cord, and lead to development of a new generation of neural prosthetics for individuals with neurological impairments.

During the eighth quarter of this contract we continued anatomical mapping of spinal neurons active during micturition, and measured the effects in the motor system of microstimulation of the lumbar spinal cord. Below each of our accomplishments is summarized.

PROGRESS IN THIS QUARTER

I. Anatomical Tracing of Genitourinary Innervation

Expression of c-fos in Genitourinary-related Spinal Neurons

The purpose of these experiments is to determine the location and rostrocaudal extent of spinal neurons that participate in control of micturition. The proto-oncogene c-*fos* that encodes the Fos protein can be induced rapidly and transiently in post-synaptic neurons by increased electrical activity. In these studies we used expression of Fos protein to identify cells within the sacral spinal cord that regulate genitourinary function in male cats.

In our previous c-fos mapping experiments we used either electrical stimulation of either the pelvic nerve or pudendal nerve (QPR 6) or reflex isometric voiding (QPR 7) to induce c-fos expression. In the present experiments we used activity arising during voiding induced by electrical stimulation of Barrington's nucleus in the pons. The results of these experiments identify neurons that were electrically active during the behavior of voiding, and thus identify spinal sites to target for microstimulation. We also began to quantify the number of cells present in different regions of the spinal cord after peripheral nerve stimulation.

METHODS

c-Fos Induced by Stimulation of Barrington's Nucleus

Sexually-intact male cats were masked with halothane (1-2% in O_2) and intubated. A venous catheter was inserted in the cephalic vein, and anesthesia maintained with α-chlorolose (Sigma, 60 mg/kg IV, supplemented at 10-15 mg/kg). Animals were respirated artificially, body temperature was maintained with a thermostatically controlled lamp, and heart rate was continuously monitored. The skin around the incision site was anesthetized using Marcaine (0.5%, 1 cc injected ID and SQ) in an effort to reduce surgically induced Fos expression. A ventral midline incision was made to expose the pre-prostatic urethra between the bladder neck and the pubic symphysis. The bladder was cannulated per-urethrally with a PE-50 catheter, and the catheter was fixed in place with a tie around the pre-prostatic urethra. The incision was closed and the catheter was connected to a pressure transducer.

The pressure in the bladder was measured using a solid state pressure transducer connected to the per-urethral bladder catheter (Deltran DPT-100, Utah Medical Products, Midvale, UT) at a bladder volume (5-10 cc) that was below the threshold for reflex micturition. The bladder volume was reduced during the two hour stimulation period if reflex contractions occurred. Recall that the ureters were intact and thus continuous bladder filling occurred during the experiment. The pressure signals were amplified, low pass filtered (fc=30 Hz), and continuously recorded on a strip chart recorder.

The dorsal aspect of the scalp was shaved and the skin around the incision site was anesthetized using Marcaine (0.5%, 1 cc injected ID and SQ). The animal was mounted in a Kopf stereotaxic frame and a craniotomy was made. Tungsten stimulating electrodes were advanced into the pons. After mapping the bladder pressure responses to microstimulation, the electrode was positioned in a region that produced micturition-like activity and stimulation was initiated (100 μs, 100 μA, 50 Hz, 2s ON 8s OFF for 2 hours).

After the period of stimulation, the animals were perfused via the aorta with saline followed by 4% paraformaldehyde in 0.1M $NaPO_4$ (pH=7.4). The brain and spinal cord were removed, stored in fixative for 2-5 days, and then transferred to 30% sucrose in 0.1M $NaPO_4$ for 2-4 days.

The sacral spinal cord was sectioned transversely at 50μm intervals on a freezing microtome. Floating sections were rinsed and exposed overnight to rabbit anti-Fos (1:10,000, Oncogene). After rinsing, sections were exposed to secondary antibody (biotinylated goat anti-rabbit) for 1 h. Fos-like immunoreactivity was visualized with the ABC method intensified with nickel chloride. Sections were rinsed, mounted on slides, dehydrated in alcohol series, cleared in xylene, and coverslipped. Slides were viewed using bright-field microscopy and locations of cells exhibiting Fos-like immunoreactivity described according to the conventions of Rexed [1954].

Quantification of the Distributions of Fos-positive Neurons

During this quarter we counted the number of cells exhibiting Fos-like immunoreactivity after electrical stimulation of either the pudendal nerve or pelvic nerve as well as in an operated, but unstimulated control. High resolution, low magnification prints were made of 3 sections from the S2 segment in each animal. The printouts were used to mark Fos-positive cells identified under higher magnifications views of the same section. The number of cells exhibiting Fos-like immunoreactivity in three different regions (fig. 2A) was averaged across 3 sections from the S2 segment in each animal.

RESULTS

c-Fos Induced by Stimulation of Barrington's Nucleus

The pattern of bladder pressure resulting from microstimulation within the dorsolateral pons is shown in fig. 1A. The large, long-latency bladder contractions had a duration that outlasted the stimulus by several seconds. In all cases the pressure returned to baseline before the next stimulus was applied. The location of the microelectrode in the brainstem is shown in fig. 1B. The large lesion was produced by a 30 s 100 μA d.c. current after the completion of the experiment, and confirms that the electrode was in Barrington's nucleus.

In all animals undergoing micturition induced by stimulation of Barrington's nucleus, nuclei exhibiting Fos-like immunoreactivity (FLI) were found bilaterally in S1-S3. The spatial distribution of Fos-positive cells was quite similar to that observed in animals that underwent a 2 h isometric micturition stimulus. Fos-positive neurons were found in the superficial dorsal horn in the lateral portion of laminae I and II, dorsal to the central canal in lamina X, and dorsolateral to the central canal in the medial part of laminae V and VI. A horizontal band of cells exhibiting FLI was found in laminae VI and VII extending from dorsal to the central canal to the intermediolateral cell column. Large numbers of Fos positive cells were identified in the intermediolateral cell column. Within this region there were 2 classes of cells: a group with large nuclei, presumably the preganglionic parasympathetic motoneurons innervating the bladder and urethra, and a group with small nuclei, presumably genitourinary-related interneurons.

Quantification of the Distributions of Fos-positive Neurons

The average number of neurons exhibiting FLI in each of the three regions of the spinal cord is plotted for four animals in fig. 2B. It is clear that electrical stimulation of the pudendal or pelvic nerve resulted in many more Fos-positive neurons than were present in the operated unstimulated control. Thus, the patterns of expression observed in the stimulated animals resulted from the specific stimulus, not the non-specific stimulus associated with the surgical procedures and instrumentation.

Electrical stimulation of either nerve resulted in a similar distribution of spinal neurons exhibiting FLI, although there were more Fos-positive neurons in region 2 (intermediolateral region) after pelvic nerve stimulation. The similarity in distribution of Fos-positive neurons is consistent with previous electrophysiological studies demonstrating that neurons in these areas receive convergent somatic and visceral afferent input [McMahon and Morrison, 1982, Honda, 1985], and previous anatomical tracing studies demonstrating parallel areas where terminals of primary afferents from the pelvic nerve and pudendal nerve have been documented [Morgan et al., 1981, Nadelhaft and Booth, 1984, Ueyama et al., 1984].

II. Microstimulation of the Lumbar Spinal Cord in Male Cats

The objective of these experiments is to map the motor responses generated about the knee joint by microstimulation of different regions of the lumbosacral spinal cord. In this series of experiments the evoked torques evoked by microstimulation were mapped, in a given rostrocaudal segment, systematically from the midline to the lateral border of the spinal cord at 250 μm intervals. Penetrations were made in rostrocaudal planes between the caudal border of the L4 segment and the middle of the L7 segment.

METHODS

Male cats were anesthetized with xylazine (Rompun, 2.0 mg/kg, SQ) and Ketamine HCl (15 mg/kg, IM), a venous catheter was inserted in the cephalic vein, and anesthesia maintained with α-chlorolose (60 mg/kg IV, supplemented at 10-15 mg/kg). Animals were intubated and respiration was maintained with a respirator. A laminectomy was made to remove the L4-L7 vertebrae. The animal was mounted in a spinal frame with pins at the hips, the head in a headholder, and vertebral clamps at L3 and S1. Body temperature was maintained between 37° and 39° C with a thermostatically controlled heat lamp, warm 5% dextrose saline with 8.4 mg/cc sodium bicarbonate added was administered IV (~20 cc/hr), and heart rate was monitored throughout the experiment. Dexamethasone (2 mg/kg, IV) was administered at the completion of the laminectomy and every 6 hours thereafter to prevent inflammation of the spinal cord.

The torques generated about the knee were measured using a custom-built strain gage instrumented beam (described in QPR #2). Torque signals were amplified, low pass filtered (fc=100 Hz), and continuously recorded on a strip chart recorder. Torques evoked by stimulation were also sampled by computer (fs=200Hz). Torques were quantified by taking the average torque during the stimulus train.

Intramuscular bipolar fine wires (stainless steel wires, 0.0018" diameter, insulated except for 2 mm at their tips) were used to record electromyograms from 4 hindlimb muscles: semimembranosus, biceps femoris, vastus medialis, and vastus lateralis. EMG signals were amplified, filtered (10 Hz-1 kHz), and sampled (2.5 kHz). Off-line, EMG signals were rectified, integrated, and the final value of the integral was used to quantify the EMG response. For each muscle, the magnitude of the rectified integrated EMG was normalized to the maximum response obtained from that muscle.

We used activated iridium wire electrodes purchased from Huntington Medical Research Institutes, Pasadena, CA (50μm Epoxylite insulated iridium wire with an exposed electrochemically determined surface area of ~225 μm^2 and a 1-3 μm tip). Stimuli were charge balanced biphasic pulses with an amplitude of 10-150 μA and a pulsewidth of 100 μs applied as 1 s to 10 s continuous trains with a frequency between 2 Hz and 100 Hz. Our standard mapping stimulus was a 1 s 20 Hz burst. Vertical, dorsal-to-ventral penetrations (increment=100-400μm) were made at multiple mediolateral locations (increment=250μm) in the middle of the lumbar segments and at intersegmental boundaries.

RESULTS

The torques evoked by microstimulation of the L6 spinal cord in two experiments is shown in figure 3. Each panel is a two dimensional map of the average knee torques evoked by microstimulation (1 s 20 Hz burst of 100 μs 100 μA pulses) as a function of the mediolateral and dorsoventral position of the microelectrode. The spatial extent of the plots parallels the region of the cord that was mapped: mediolateral zero corresponds to the midline, dorsoventral zero corresponds to the cord surface at the midline, and the grids on the axes indicate the intervals at which mapping stimuli were applied (200 μm depth interval, 250 μm mediolateral interval). The evoked torques are plotted as greyscale values with flexion towards black, extension towards white, and zero net torque as grey.

There was a strong congruence between the spatial patterns of torque generation measured in the two experiments. Also, although the first example had larger absolute torque magnitudes, the relative magnitudes of the flexion and extension torques were similar across the two experiments. The maximum extension torque was approximately twice the maximum flexion torque in both cases.

Stimulation in the dorsal aspect of the cord, in a region corresponding to the dorsal root entry zone, produced strong flexion torques. As reported previously, the pattern and magnitude of these responses was strongly dependent on stimulus frequency. The 20 Hz mapping stimulus produced a strong onset response followed by a decay to a lower value after the first few pulses in the 1 s train. Flexion torques were also produced by microstimulation at the lateral aspect of the intermediate region. In the lateral ventral horn, microstimulation produced strong extension torques, while microstimulation at more ventral and medial locations produced flexion torques. These results document the motor responses generated by intraspinal microstimulation, and demonstrate that the effects of spinal microstimulation are reproducible across experiments.

The torques produced by microstimulation varied with rostrocaudal segment. Figure 4A shows a map measured at L7 in the same animal as the L6 map in fig. 3B. As in the maps at L6, microstimulation in central regions of the dorsal aspect of the spinal cord produced strong flexion torques, and stimulation in the lateral aspect of the intermediate aspect produced weaker flexion torques. In the ventral aspect of the cord, stronger flexion torques were produced by microstimulation over a larger area than in L6. Extension torques were produced at locations in the ventral aspect of the cord that were lateral to locations producing flexion torques.

Suprisingly, at both L6 and L7, there was a large area in the intermediate region of the cord which produced no torques. Anatomical and electrophysiological studies have documented large numbers of different classes of motor system interneurons in this area [Jankowska, 1992]. The lack of response from these neurons may be due to the anesthesia (α-chlorolose) or the result of their state-dependent effects within the motor system.

These data provide maps of the net motor response produced by microstimulation. However, it is important also to consider the activation level of the individual muscles that are contributing to the net torque. This information is necessary to evaluate the presence of co-contraction of either agonist or antagonist muscles. Toward this end we recorded electromyograms in four muscles, a medial flexor semimembranosus, a lateral flexor biceps femoris, a medial extensor vastus medialis and a lateral extensor vastus lateralis, as well as recording isometric joint torque.

Figure 4B shows the magnitude of the rectified integrated electromyograms (riEMG) as a function of the mediolateral and dorsoventral position of the microelectrode in the L7 spinal cord. The amplitude of the rectified integrated EMG (riEMG) was normalized by the maximum response obtained for each muscle. There was a clear correspondence between the maps of knee torque and the maps of riEMG for the four muscles. These maps demonstrate that both semimembranosus and biceps femoris contribute to the flexion torques produced by microstimulation in the dorsal aspect of the cord, and that at these locations there was no co-activation of the extensor muscles. In the intermediate area, the biceps femoris was more active than the semimembranosus and again there was no co-activation of the extensors. Similar regions in the ventral horn generated activation of both semimembranosus and biceps femoris, although semimembranosus was more active. These data also show that the vasti are co-activated over the same region of the lateral ventral horn, and that this region is distinct from the areas producing activation of the flexors.

Mapping the motor responses generated by microstimulation of the lumbar spinal cord revealed a rostrocaudal and mediolateral segregation between regions which generated activation of flexors and extensors. This spatial segregation is in accord with the classical maps generated by Romanes using cell chromatolysis [Romanes, 1951], as well as the results of a recent study which employed HRP to map the somatic innervation of the hindlimb muscles in the cat [Vanderhorst and Holstege, 1997]. This spatial segregation enabled selective activation of flexor and extensor muscles using intraspinal microstimulation which was assessed using EMG recordings.

Both flexion and extension torques were produced by direct activation of spinal motoneurons in the ventral aspect of the cord, and flexion torques were also produced indirectly by stimulation within the dorsal and lateral intermediate areas. These locations also produced extension of the contralateral hindlimb, which was noted, but not quantified. Thus, stimulation of the dorsal aspect of the cord appears to generate electrically two classical spinal reflexes: flexion withdrawal and crossed extension. Interestingly, stimulation in the intermediate laminae produced little motor response in the muscles which we were transducing.

REFERENCES

Honda, C.N. (1985) Visceral and somatic afferent convergence onto neurons near the central canal in the sacral spinal cord of the cat. J. Neurophysiology 53:1059-1078.

McMahon, S.B., J.F.B. Morrison (1982) Two groups of spinal interneurons that respond to stimulation of the abdominal viscera of the cat. J. Physiol. 322:1-20.

Morgan, C., I. Nadelhaft, W.C. de Groat (1981) The distribution of visceral primary affferents from the pelvic nerve to Lissauer's tract and the spinal grey matter and its relationship to the sacral parasympathetic nucleus. J. Comp. Neurol 201:415-440.

Nadelhaft, I., A.M. Booth (1984) The location and morphology of preganglionic neurons and the distribution of visceral afferents from the rat pelvic nerve: a horseradish peroxidase study. J. Comp. Neurol. 226:238-245.

Rexed, B. (1954) A cytoarchitectonic atlas of the spinal cord in cat. J. Comp. Neurol. 100:297-351.

Romanes, G.J. (1951) The motor cell columns of the lumbo-sacral spinal cord of the cat. J. Comp. Neurol. 94:313-358.

Ueyama, T., N. Mizuno, S. Nomura, A. Konishi, K. Itoh, H. Arakawa (1984) Central distribution of afferent and efferent componenets of the pudendal nerve in cat. J. Comp. Neurol. 222:38-46

Vanderhorst, V.G.J.M., G. Holstege (1997) Organization of lumbosacral motoneuronal cell groups innervating hindlimb, pelvic floor, and axial muscles inthe cat. J. Comp. Neurol. 382:46-76.

OBJECTIVES FOR THE NEXT QUARTER

I. Anatomical Tracing of the Genitourinary and Hindlimb Motor Systems

We will complete counting to quantify the location and rostrocaudal extent of c-Fos positives neurons after genitourinary stimuli.

We will initiate a study using spinally injected retrograde tracers to map the location and rostrocaudal extent of last order interneurons that project to motoneurons.

III. Microstimulation of the Lumbosacral Spinal Cord

We will continue experiments to map systematically the motor responses generated by microstimulation of the lumbar spinal cord.

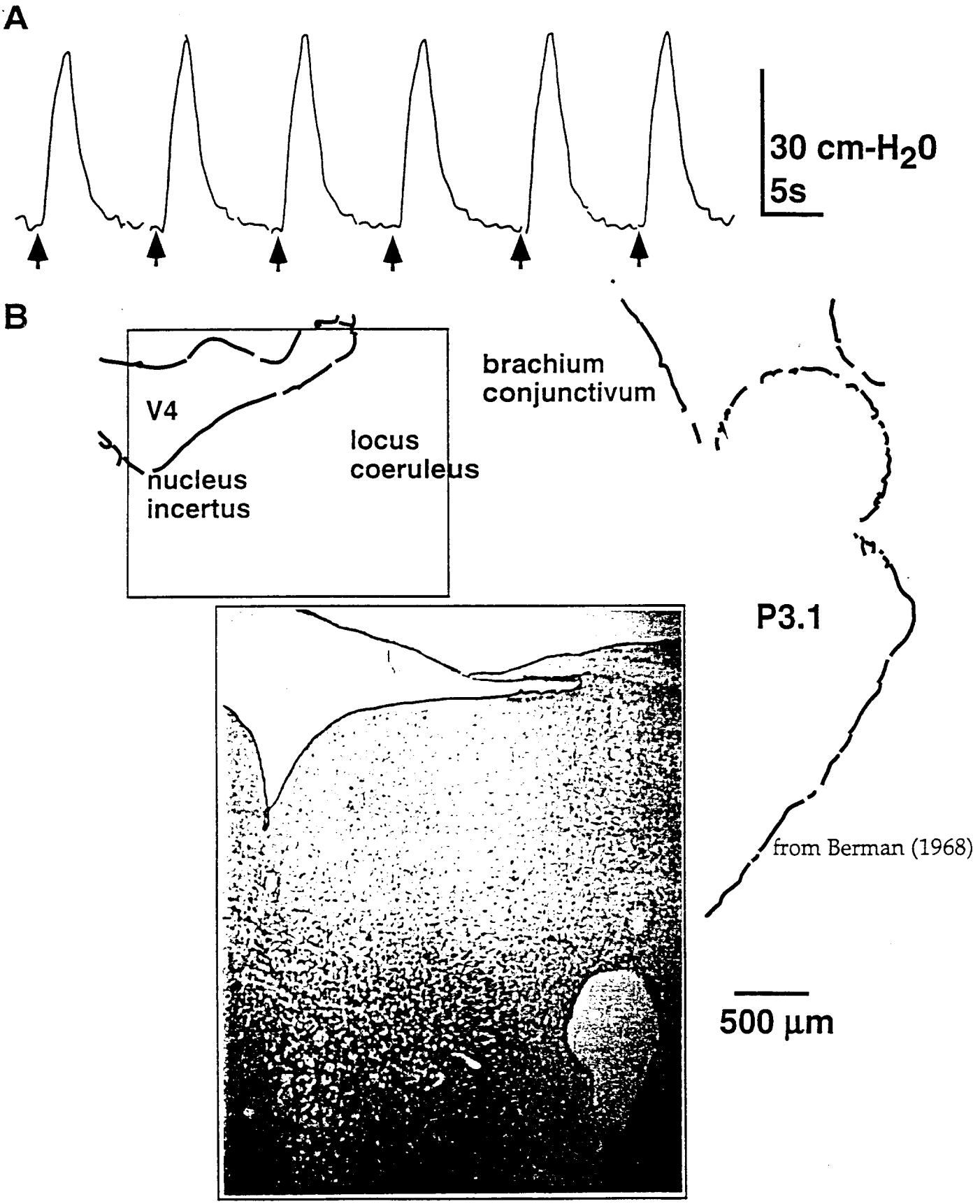

Figure 1: Micturition-like activity evoked by pontine stimulation. A.) Patterns of bladder pressures recorded during microstimulation of Barrington's nucleus (100 µA, 50 Hz, 2 s ON, 8 s OFF, onset indicated by arrows). B.) Photomicrograph of lesion made after stimulation and line drawing illustrating that the microelectrode was within Barrington's nucleus.

A

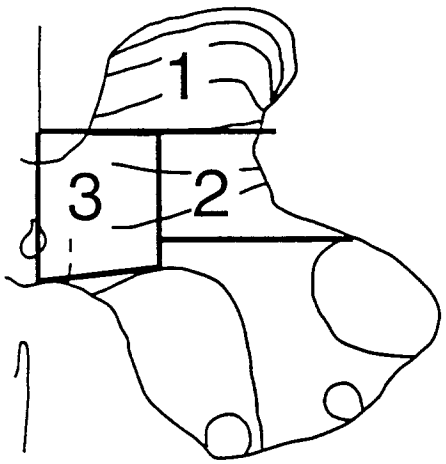

from Rexed (1954)

B

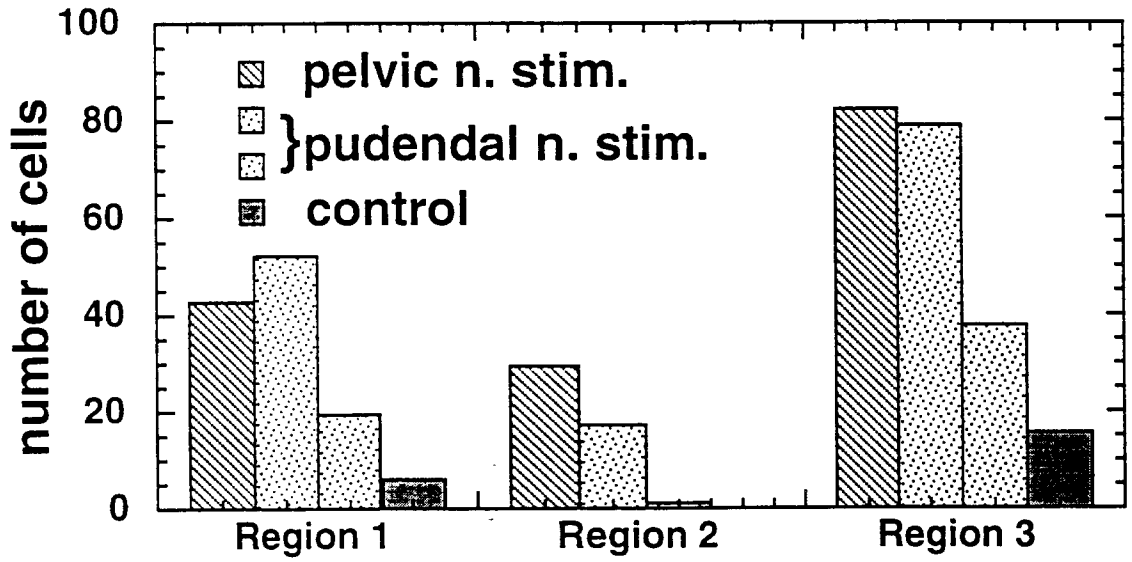

Figure 2: Quantification of the distributions of Fos-positive neurons resulting from electrical stimulation of either the pudendal nerve or the pelvic nerve. A.) Diagram showing the relationship of the three regions to Rexed's laminae in S2. B.) Histogram of the number of cells in each region (average from 3 sections in S2) in 4 animals.

Figure 3: ON PAGE 11
Maps of Motor Responses Generated by Microstimulation of the L6 Spinal Cord
Two dimensional maps of the knee torques evoked by microstimulation of the lumbar spinal cord (1 s 20 Hz burst of 100 μs 100 μA pulses). Each panel is a 2-dimensional map of the spinal cord at the middle of L6 from two different animals (A, B). Mediolateral zero corresponds to the midline, and dorsoventral zero corresponds to the cord surface at the midline. The evoked extension or flexion torques are plotted as greyscale values.

Figure 4: ON PAGE 12
Maps of Motor Responses Generated by Microstimulation of the L7 Spinal Cord
(A) Two dimensional map of the isometric knee torque evoked by microstimulation of the L7 spinal cord (1 s 20 Hz burst of 100 μs 100 μA pulses). The evoked extension or flexion torques are plotted as greyscale values. (B) Two dimensional maps of the rectified integrated EMG in four muscles. The magnitude of the riEMG was normalized to maximum by muscle and is plotted as a greyscale value. In both A and B mediolateral zero corresponds to the midline, and dorsoventral zero corresponds to the cord surface at the midline.

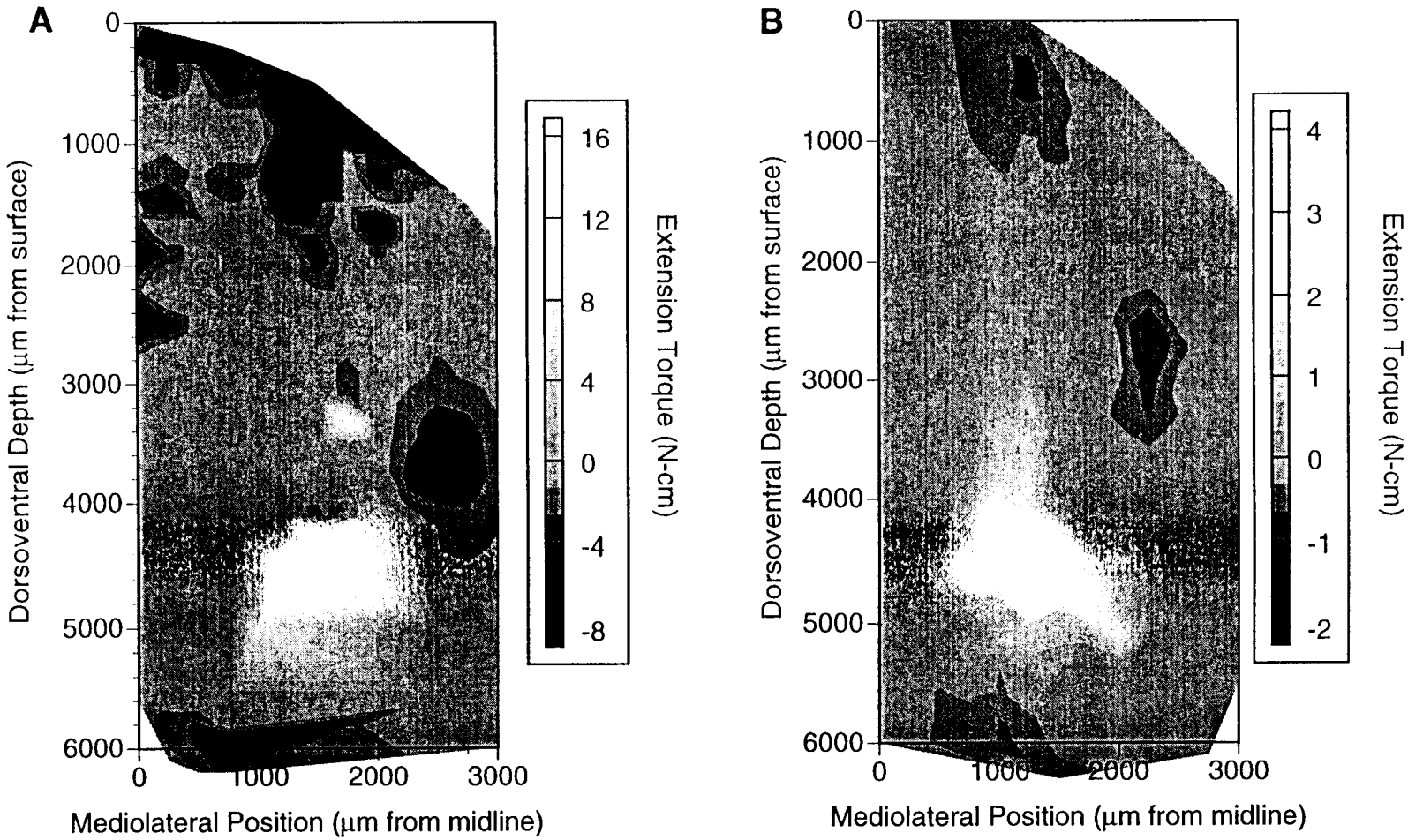
A
0
1000
2000
3000
4000
5000
6000
Dorsoventral Depth (µm from surface)
0
1000
2000
3000
Mediolateral Position (µm from midline)
16
12
8
4
0
-4
-8
Extension Torque (N-cm)
B
0
1000
2000
3000
4000
5000
6000
Dorsoventral Depth (µm from surface)
0
1000
2000
3000
Mediolateral Position (µm from midline)
4
3
2
1
0
-1
-2
Extension Torque (N-cm)

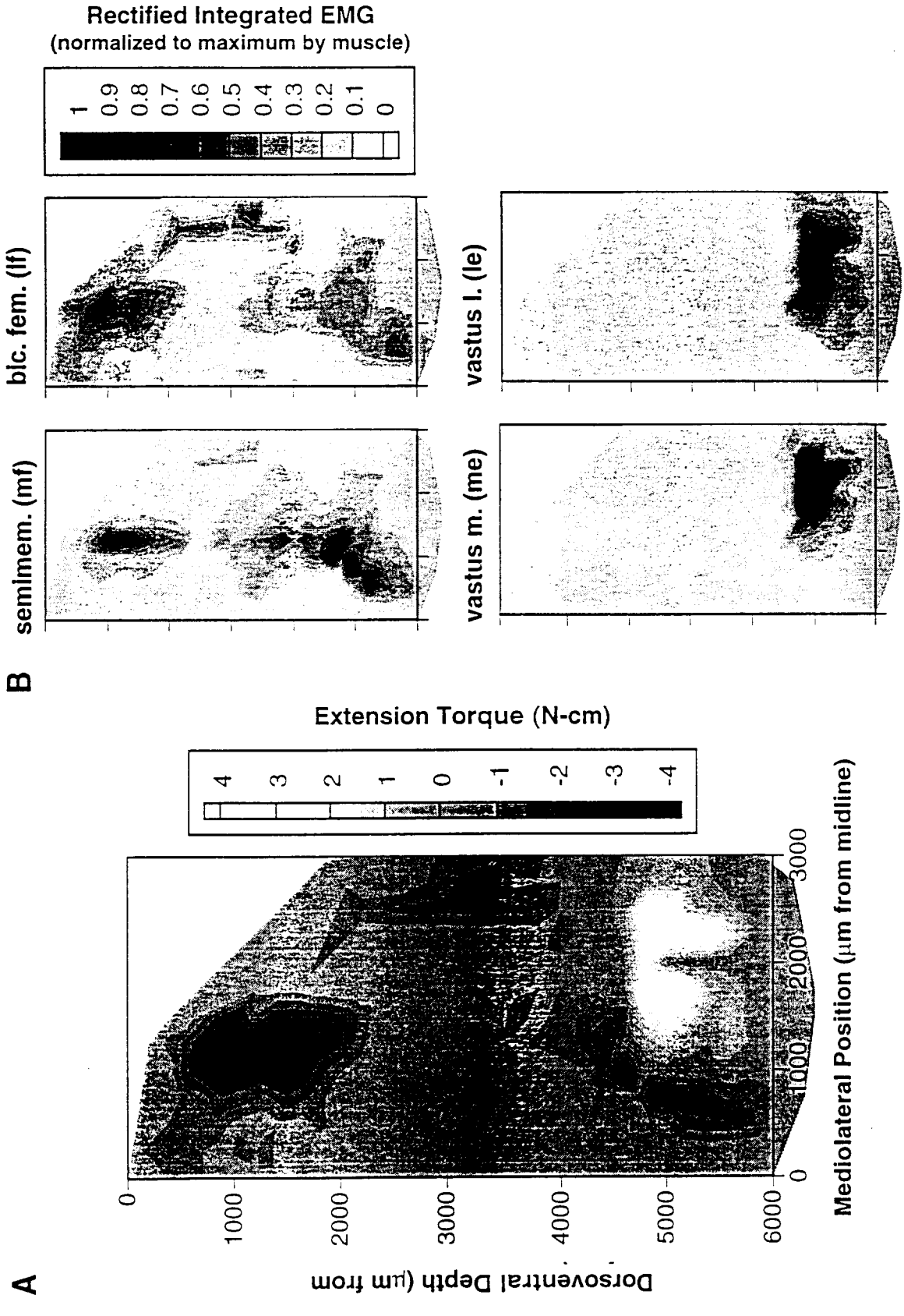
A
Extension Torque (N-cm)
4
3
2
1
0
-1
-2
-3
-4
Dorsoventral Depth (μm from
0
1000
2000
3000
4000
5000
6000
Mediolateral Position (μm from midline)
0
1000
2000
3000
B
Rectified Integrated EMG
(normalized to maximum by muscle)
1
0.9
0.8
0.7
0.6
0.5
0.4
0.3
0.2
0.1
0
semimem. (mf)
blc. fem. (lf)
vastus m. (me)
vastus l. (le)